# Supplementary Information for:

## Fluorine-18 labeled poly (ADP-ribose) polymerase1 inhibitor as a potential alternative to 2-deoxy-2-[$^{18}$F]fluoro-D-glucose positron emission tomography in oral cancer imaging.

Abbreviated title: [$^{18}$F]PARPi imaging as a potential alternative to [$^{18}$F]FDG PET/CT in oral cancer imaging.

Paula Demétrio De Souza França, MD[a,b], Sheryl Roberts, PhD[a], Susanne Kossatz, PhD[a,1], Navjot Guru[a], Christian Mason, PhD[a], Daniella Karassawa Zanoni, MD[b,2], Marcio Abrahão, MD,PhD[b], Heiko Schöder, MD,MDA[a], Ian Ganly, MD,PhD[c,d], Snehal G. Patel, MD[c,d,*], Thomas Reiner, PhD[a,d,e,*]

[a] Department of Radiology, Memorial Sloan Kettering Cancer Center, New York, NY, USA.
[b] Department of Otorhinolaryngology and Head and Neck Surgery, Federal University of São Paulo, SP, Brazil.
[c] Department of Surgery, Memorial Sloan Kettering Cancer Center, New York, NY, USA.
[d] Weill Cornell Medical College, New York, NY, USA.
[e] Chemical Biology Program, Memorial Sloan Kettering Cancer Center, New York, NY, USA.
[1]Additional affiliation: Department of Nuclear Medicine, School of Medicine, Technische Universität München, Munich, Germany.
[2] Additional affiliation: Department of Radiology, University of Iowa, IA, USA.

**Correspondence addressed to:**

**Snehal Patel* - 1275 York Avenue. New York, NY, 10065. patels@mskcc.org; (P) 1-646-888-3461; (F) 917-432-2111

**Thomas Reiner* - 1275 York Avenue. New York, NY, 10065. reinert@mskcc.org; (P) 1-646-888-3461; (F) 646 4220408

## General methods

All reactions were magnetically stirred, and room temperature refers to 20–25 °C. High performance liquid chromatography (HPLC) purification and analysis was performed on a Shimadzu UFLC HPLC system equipped with a DGU-20A degasser, an SPD-M20A UV detector, a LC-20AB pump system, and a CBM-20A communication BUS module. A LabLogic Scan-RAM radio-TLC/HPLC-detector was used for the radioactive signal. HPLC solvents (Buffer A: 0.1% TFA in water, Buffer B: 0.1% TFA in MeCN) were filtered before use. HPLC purification and analysis of PARPi-FL was performed on an analytical column reversed-phase Atlantis® T3 5 µm column (C18, 4.6 mm, and 250 mm). HPLC purification and analysis of [$^{18}$F]PARPi was performed on a semi-preparative reversed-phase Phenomenex Gemini column (C6-Phenyl, 5 µm, 10 mm, and 250 mm). Purification and analysis of PARPi-FL was performed with Method A (flowrate: 1.0 mL min$^{-1}$; gradient: 0–15 min 5%–95% B; 15–18 min 95% B; 18–18.3 min 95-5% B). Purification and analysis of [$^{18}$F]PARPi was performed with Method B (flowrate: 5 mL min$^{-1}$; isocratic: 0–45 min 30% B). All PET imaging experiments were conducted on a microPET INVEON camera equipped with a CT scanner (Siemens, Knoxville, TN). Digital phosphor autoradiography was obtained using a Typhoon FLA 7000 laser scanner from GE Healthcare (Port Washington, NY). A lyophilizer (FreeZone 2.5 Plus, Labconco, Kansas City, MO, USA) was used for freeze drying. An automated cell counter (Beckman Coulter, Vi-Cell viability analyzer) was used for counting the number of cells. Tissues were sectioned using a Avantik, QS11 cryotome (Belair, New Jersey, USA). *In vitro* fluorescence confocal microscopy on cells was carried out using a LSM880 Airyscan confocal microscope (Zeiss, Germany). QMA light ion-exchange cartridges and C-18 Sep-Pak light cartridges were obtained from Waters (Milford, MA).

## Chemicals

Commercially available compounds were used without further purification unless otherwise stated. 4,7,13,16,21,24-Hexaoxa-1,10-diazabicyclo[8.8.8]hexacosane ($K_{222}$), extra-dry dimethyl sulfoxide (DMSO) over molecular sieves, Bio Ultra PEG 500, Ethyl 4-nitrobenzoate, potassium carbonate ($K_2CO_3$), triethylamine ($NEt_3$), trifluoroacetic acid (TFA) and 4-Fluorobenzoic acid were purchased from Sigma-Aldrich (St. Louis, MO). [$^{18}$F]FDG was obtained from the Memorial Sloan Kettering Cancer Center (MSK) Radiochemistry and Molecular Imaging Probes Core. HPLC and LC-MS grade acetonitrile (MeCN) were obtained from Fischer scientific (Hampton, NH). Water (> 18.2 MΩ cm$^{-1}$ at 25 °C) was obtained from an Alpha-Q Ultrapure water system

from Millipore (Bedford, MA). PARP-NH precursor (4-(4-fluoro-3-(piperazine-1-carbonyl)benzyl)phthalazin-1(2H)-one) was purchased from AA blocks (San Diego, CA) and purified by HPLC using Method A before use and further synthesis. BODIPY-FL NHS-ester was purchased from Invitrogen, Carlsbad, CA without further purification. PARPi-FL was kept as a 1.5 mM stock solution in BioUltra PEG300 and diluted to the final working concentration for the respective *in vitro* experiments with full cell medium.

**PARPi-FL synthesis**

The synthesis of PARPi-FL was prepared according to our previously described procedures [1-3]. Briefly, fluorescent dye BODIPY-FL NHS-ester (1.0 equivalent) was conjugated to 4-(4-fluoro-3-(piperazine-1-carbonyl)benzyl) phthalazin-1(2H)-one (1.0 equivalent) under a base, $Et_3N$ (5.0 equivalent) in acetonitrile for 4 h at room temperature and purified by preparative HPLC (Atlantis® T3 5 µm column 4.6 × 250 mm, 1 mL/min, 5 to 95% of acetonitrile in 15 min) to afford PARPi-FL in 70–79% yield as a red solid. Analytical HPLC analysis (Waters' Atlantis T3 C18 5 µm 4.6 × 250 mm column) showed high purity (> 99%, $t_R$ = 13.9 min) of the imaging agent. The identity of PARPi-FL was confirmed using ESI-MS (MS(+) *m/z* = 663.63 $[M + Na]^+$).

**[$^{18}$F]PARPi radiosynthesis**

[$^{18}$F]PARPi was synthesized using an optimized labeling procedure according to our previously described method [3-6]. Briefly, [$^{18}$F] fluoride was obtained via the $^{18}O(p,n)^{18}F$ nuclear reaction of 16.5-MeV protons in a GE Healthcare PET Trace 800 using enriched $^{18}$O-water. A QMA cartridge containing cyclotron-produced [$^{18}$F]fluoride (50 mCi, 2.22 GBq) was eluted with a 2 mL solution of $K_{222}/K_2CO_3$ (Kryptofix [2.2.2] (4,7,13,16,21,24-hexaoxa-1,10-diazabicyclo [8.8.8]hexacosane, (22.5 mg)), 0.02 mL 5 M $K_2CO_3$ and 4% MeCN in $H_2O$ in $V_{total}$ = 5 mL). Solvents were removed azeotropically at 120 °C under $N_2$. Afterwards, 500 µg of ethyl-4-nitrobenzoate in 100 µL of dry DMSO was added and the mixture heated to 150 °C for 15 min. 50 µL of 1M NaOH was added followed by 50 µL of 1M HCl. Then, 2 mg of 4-(4-fluoro-3-(piperazine-1-carbonyl)benzyl) phthalazin-1(2H)-one in dry DMSO 100 µL was added followed by 10 mg of HBTU dissolved in 100 µL of DMSO and 20 µL of $Et_3N$. 400 µL of MeCN and 1 mL $H_2O$ was added to the mixture and the product purified by reverse phase Prep-HPLC (Method B, $t_R$ = 31. 22 min) yielding (non-decay-corrected) 21% ± 3.0%. The radiochemical purity showed > 98% and the molar activity is 37,000 MBq/µmol (1.0 Ci/µmol).

**Cell lines and cell culture**

FaDu and Cal 27 cell lines were purchased from ATCC, Manassas, VA. Cells were grown in a monolayer culture at 37 °C in a 5% $CO_2$ humidified atmosphere. FaDu cells were maintained in MEM and Cal 27 in D-MEM medium. Both media contained 10% (v/v) FBS and 1% PenStrep. Both cell lines tested negative for mycoplasma infection. Cell lines were tested for PARP1 expression and PARPi-FL uptake prior to xenografting.

**PARPi-FL cell staining and confocal imaging**

To determine PARPi-FL uptake *in vitro*, we plated 250,000 cells of either FaDu or Cal 27 in different chambers of an 8-well chamber plate (Thermo Fisher Scientific, 06171480, USA). Cells were allowed to attach and grow for 24 hours. Cells were incubated with PARPi-FL (100 nM in 30% PEG300/PBS) for 5 minutes before being washed in PBS for 5 minutes. A solution with 10% Hoechst in PBS was added into each well for 5 more minutes and washed out with PBS for 5 minutes. PBS was again added, and the live cells were imaged, in an 8-well chamber, using a Confocal Microscope (LMS800, Zeiss, Germany). Images were acquired at 488 nm and 543 nm excitations wavelengths.

**Western blot**

PARP1 protein expression was measured in FaDu and Cal 27 cell lysates using Western blot analysis as described in previous papers [7]. Briefly, proteins were isolated from cells and 20 µg of protein per sample were separated with SDS/PAGE gel electrophoresis and transferred to a nitrocellulose membrane. Proteins were detected using antibodies specific for PARP1 (1:1,000, Invitrogen; PA5-16452) and β-actin (1:40,000; Cell Signaling Technology; 3700) with a corresponding horseradish peroxidase (HRP) conjugated secondary antibody (1:20,000, ab6721, Abcam, USA). Detection was performed using a chemiluminescent substrate (Thermo Scientific #34077, Super Signal West Pico, USA). The bands were visualized using an automated blot processing machine (Ewen-Parker X-Ray corporation, New York, USA) with a light sensitive clear blue x-ray film (Thermo Scientific, 24x30 cm, SB2324231, Belgium) with 30 seconds exposure time.

**H&E staining of tissue sections**

After autoradiography, slides were fixed in 4% paraformaldehyde (PFA, MP Chemicals, Solon, OH) in sterile water for 10 minutes at 4 °C and kept for 10 minutes in 70% ethanol. The sections were stained with hematoxylin and eosin (H&E) by the MSK Molecular Cytology Core facility.

Slides were scanned (Mirax, 3DHISTECH, Budapest, Hungary) to allow for digital histological correlation with autoradiography data.

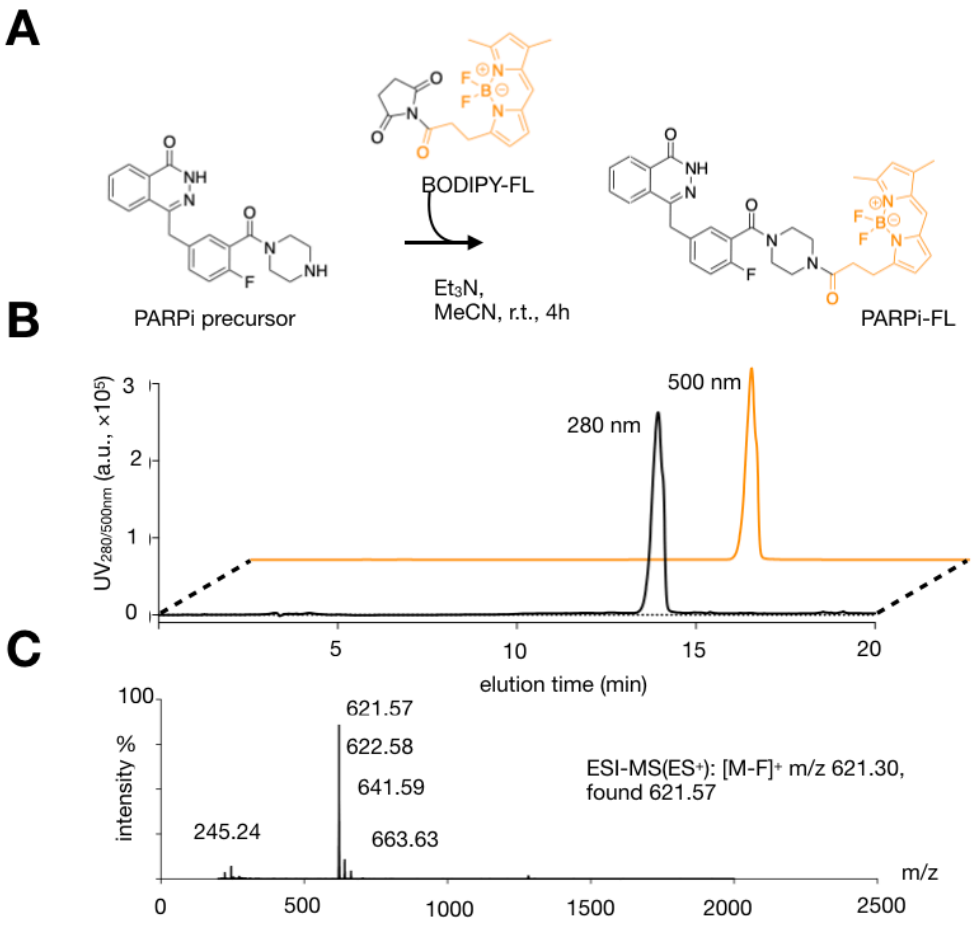


Supplementary Fig. 1. Chemical characterizations of PARPi-FL. (A) Scheme for the synthesis of PARPi-FL by conjugating PARPi precursor to BODIPY. *Reagents and conditions*: anhydrous MeCN, $Et_3N$, 4 h, r.t, 70%. (B) HPLC spectra from 0–20 minutes at 280 nm (*black*) and 500 nm (*orange)* of PARPi-FL (> 99% purity). (C) ESI-MS chromatogram of PARPi-FL.

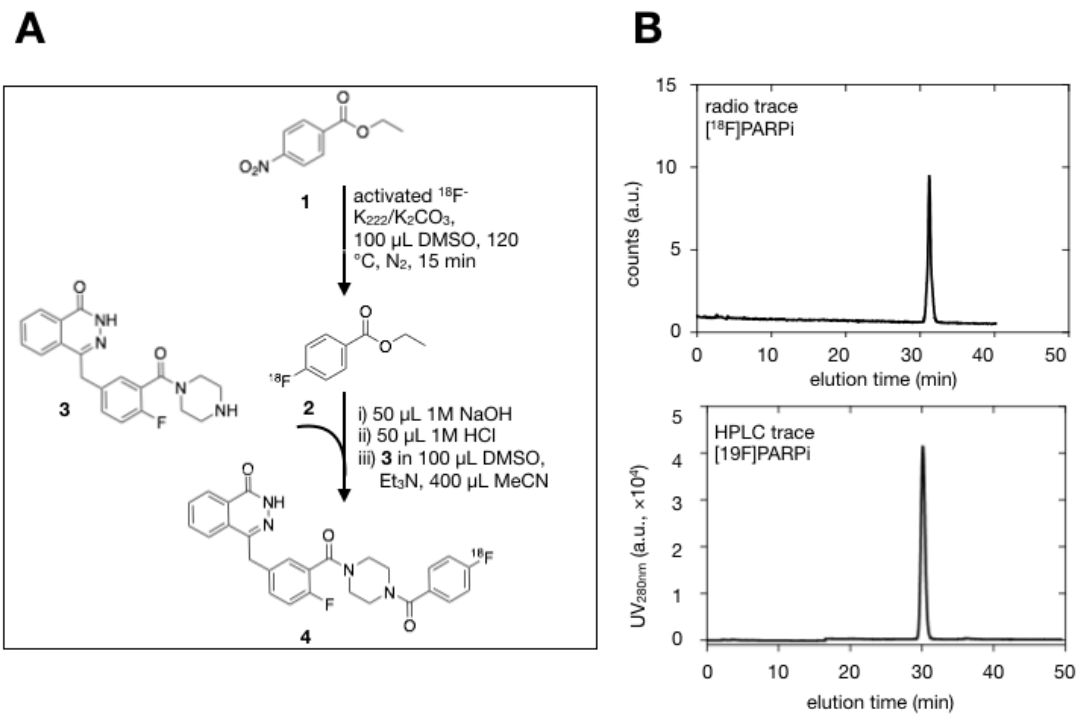


Supplementary Fig. 2. Chemical characterization of [$^{18}$F]PARPi. **(A)** Scheme for the two-step synthesis of [$^{18}$F]PARPi (compound **4**) . *Reagents and conditions*: Reaction 1: ethyl 4-nitrobenzoate (compound **1**), activated $F^-$, $K_{222}/K_2CO_3$, DMSO, 120 °C, $N_2$, 15 min. Reaction 2: Compound **3**, 50 µL 1M NaOH, 50 µL 1M HCl, DMSO, $Et_3N$. **(B)** The radiotrace chromatogram (*top*) and HPLC trace at 280 nm (*bottom*) of [$^{18}$F]PARPi.

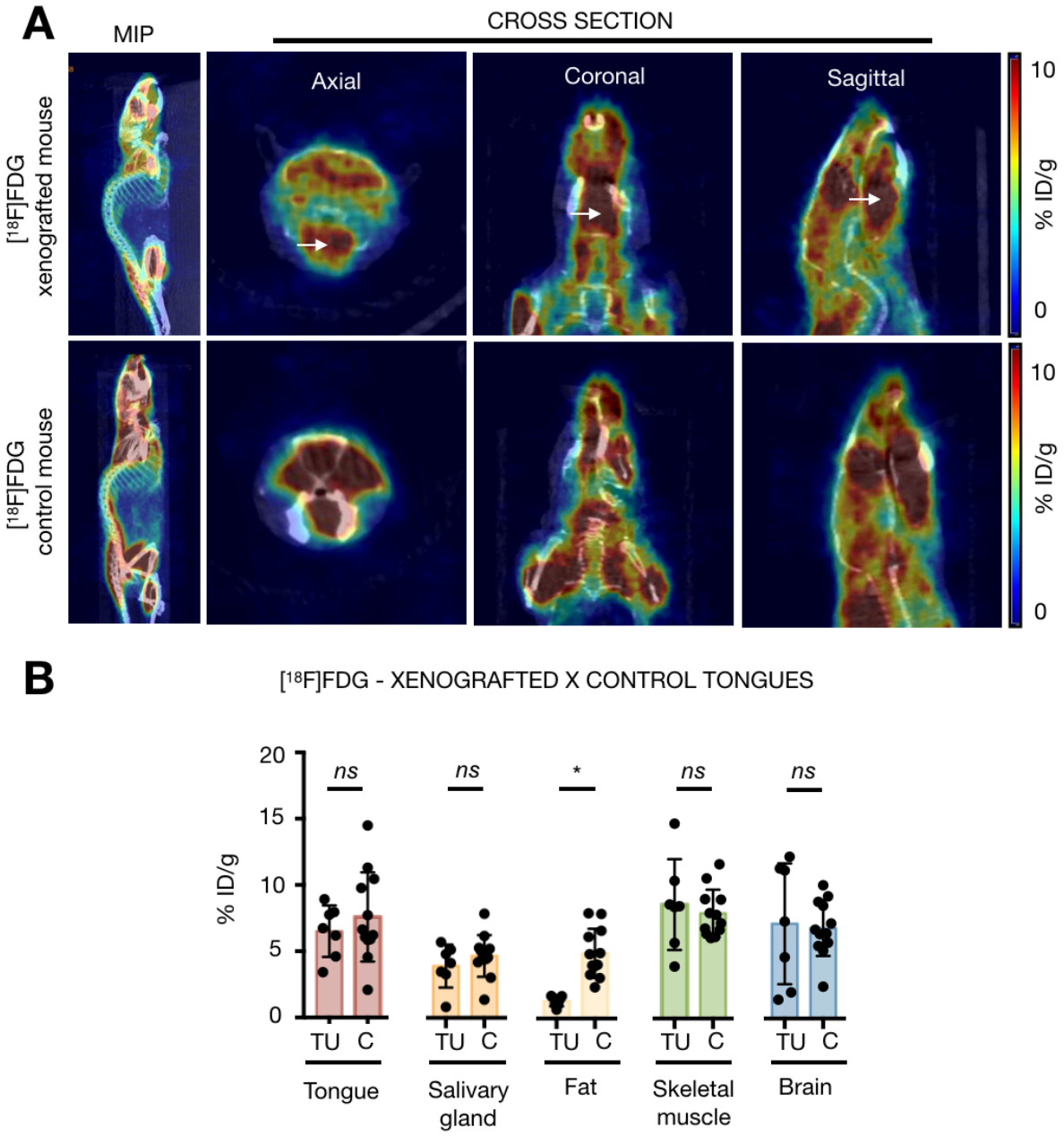


Supplementary Fig. 3. PET imaging with [$^{18}$F]FDG. Xenografted groups of animals were inoculated on the anterior 1/3 and ventral portion of the right-hand side of the tongue with 500,000 cancer cells in 20 µL of PBS (n = 3 FaDu, n = 4 Cal 27), and tumors were allowed to proliferate for 4 weeks. Twelve healthy nude mice were used as controls. All animals were injected with an average of 7.7 ± 2.2 MBq (208.1 ± 59.4 µCi) of [$^{18}$F]FDG on Day 1 after tumor

establishment and imaged for 15 minutes on an INVEON small-animal micro-PET/CT scanner under isoflurane-induced anesthesia. **(A)** Representative images of the PET/CT scans taken from a tumor-bearing and a control mouse on Day 1. The top row: mouse with tongue orthotopic tumor, bottom row: healthy control mouse. Arrows point to the tumor. Images show similar uptake of [$^{18}$F]FDG in both tumor-bearing and control mice. [$^{18}$F]FDG scans showed high physiological uptake in the tongue, floor of mouth, and masticatory muscles. **(B)** Quantification of the tracer uptake in different organs from PET/CT images. Statistical analysis was performed using the Mann Whitney test in GraphPad Prism 7. Data points represent mean values, and error bars represent standard deviations. [$^{18}$F]FDG quantification showed that the uptake in tumor was not significantly different from the other organs, except for fat (*$p < 0.05$).

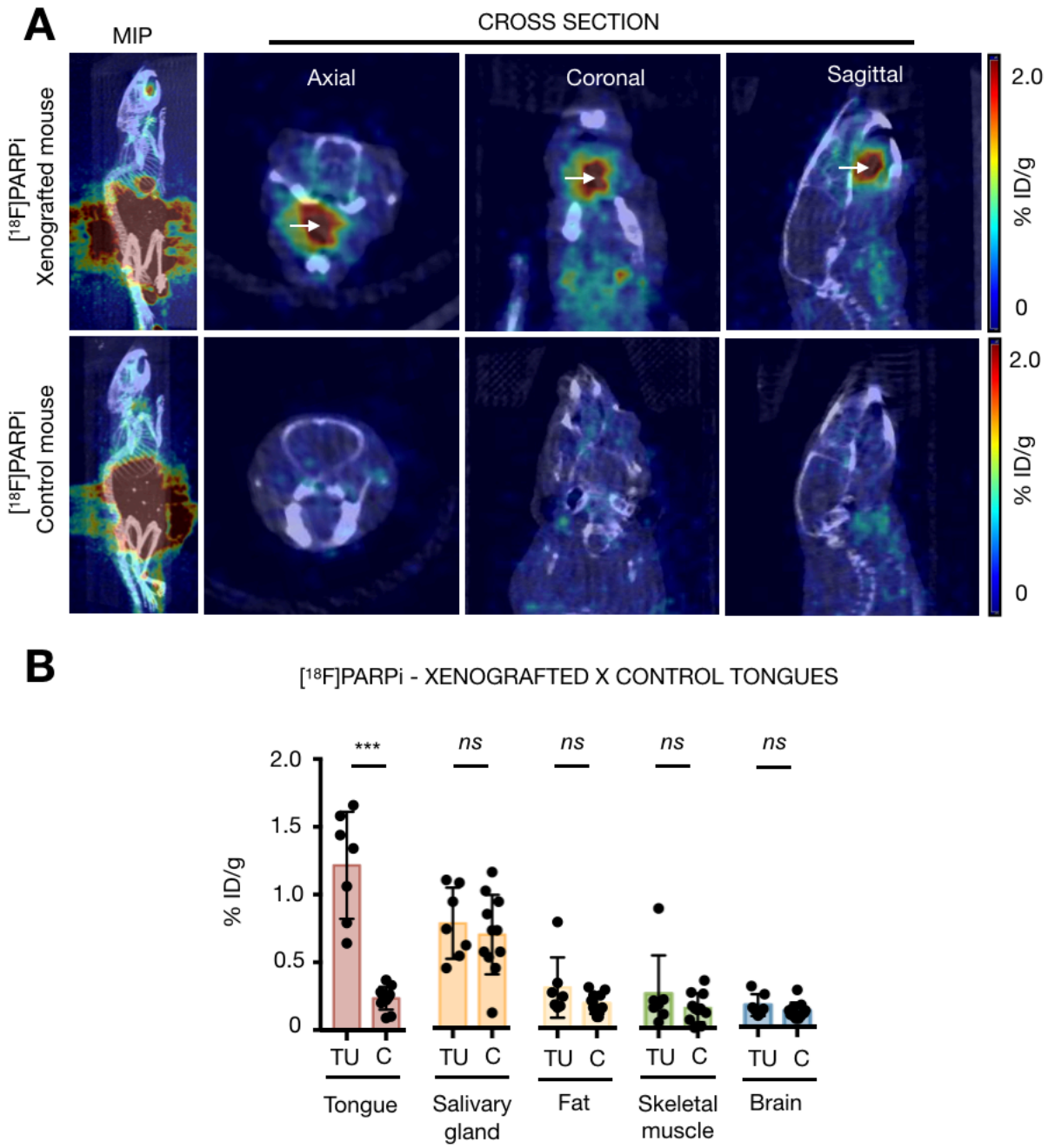


Supplementary Fig. 4. PET imaging with [$^{18}$F]PARPi. Xenografted group of animals were inoculated on the anterior 1/3 and ventral portion of the right-hand side of the tongue with 500,000 cancer cells in 20 µL of PBS (n = 3 FaDu, n = 4 Cal 27), and tumors were allowed to proliferate for 4 weeks. Twelve healthy nude mice were used as controls. All animals were

injected with an average of 10.4 ± 3 MBq (282.2 ± 80.6 μCi) of [$^{18}$F]PARPi on Day 2 after tumor establishment and imaged on an INVEON small-animal micro-PET/CT scanner under isoflurane-induced anesthesia for 15 minutes. **(A)** Representative images of the PET/CT scans taken from a tumor-bearing and a control mouse on Day 2. The top row: mouse with tongue orthotopic tumor, bottom row: healthy control mouse. Arrows point to the tumor. Images show clear tumor delineation with [$^{18}$F]PARPi with almost no uptake in controls. **(B)** Quantification of the tracer uptake in different organs from PET/CT images. Statistical analysis was performed using the Mann Whitney test in GraphPad Prism 7. Data points represent mean values, and error bars represent standard deviations. [$^{18}$F]PARPi quantification showed that the uptake in tumor was significantly higher than all the other organs (*$p > 0.05$).

**References**

[1] Reiner T, Lacy J, Keliher EJ, Yang KS, Ullal A, Kohler RH, et al. Imaging therapeutic PARP inhibition in vivo through bioorthogonally developed companion imaging agents. Neoplasia (New York, N.Y.) 2012;14:169-77.
[2] Irwin CP, Portorreal Y, Brand C, Zhang Y, Desai P, Salinas B, et al. PARPi-FL--a fluorescent PARP1 inhibitor for glioblastoma imaging. Neoplasia (New York, N.Y.) 2014;16:432-40.
[3] Carney B, Kossatz S, Lok BH, Schneeberger V, Gangangari KK, Pillarsetty NVK, et al. Target engagement imaging of PARP inhibitors in small-cell lung cancer. Nature communications 2018;9:176.
[4] Carney B, Carlucci G, Salinas B, Di Gialleonardo V, Kossatz S, Vansteene A, et al. Non-invasive PET Imaging of PARP1 Expression in Glioblastoma Models. Molecular imaging and biology : MIB : the official publication of the Academy of Molecular Imaging 2016;18:386-92.
[5] Kossatz S, Carney B, Schweitzer M, Carlucci G, Miloushev VZ, Maachani UB, et al. Biomarker-Based PET Imaging of Diffuse Intrinsic Pontine Glioma in Mouse Models. Cancer research 2017;77:2112-23.
[6] Tang J, Salloum D, Carney B, Brand C, Kossatz S, Sadique A, et al. Targeted PET imaging strategy to differentiate malignant from inflamed lymph nodes in diffuse large B-cell lymphoma. Proceedings of the National Academy of Sciences of the United States of America 2017;114:E7441-e9.
[7] Kossatz S, Carney B, Farley C, Weber WA, Drain CM, and Reiner T. Direct Imaging of Drug Distribution and Target Engagement of the PARP Inhibitor Rucaparib. Journal of nuclear medicine : official publication, Society of Nuclear Medicine 2018;59:1316-20.